PHYSICAL REVIEW A **70**, 011404(R) (2004)

High-order harmonic generation from two-center molecules: Time-profile analysis of nuclear contributions

G. Lagmago Kamta and A. D. Bandrauk
Laboratoire de Chimie Théorique, Faculté des Sciences, Université de Sherbrooke, Sherbrooke, Québec, Canada, J1K 2R1
(Received 27 March 2004; published 30 July 2004)

We solve the exact three-dimensional time-dependent Schrödinger equation for H_2^+ (with fixed nuclei) interacting with an intense laser pulse with an arbitrary oriented linear polarization. We find that at equilibrium internuclear distance, the ionization probability of H_2^+ is maximum for the parallel orientation of the molecule with respect to the laser polarization, and is minimum for the perpendicular orientation. The contribution of each nucleus to the harmonic spectrum is evaluated, so that interference effects between the two contributions are assessed unambiguously. We show that every half-cycle, high order harmonics are emitted by each nucleus when the electron wave packet returns for a recollision with both nuclei, and that the resulting harmonic emission is predominant for the nucleus that experiences the first recollision. In general, each nucleus emits both even and odd harmonics, but even harmonics are destroyed by interferences between contributions from each nucleus. In general, this destructive interference occurs over a large spread of harmonic orders, which depends on the angle between the molecular axis and the laser polarization.

DOI: 10.1103/PhysRevA.70.011404 PACS number(s): 42.50.Hz, 33.80.−b, 42.65.Ky

Coherent radiation at high frequency can be produced via high-order harmonic generation (HOHG), which occurs when atoms or molecules, subjected to intense laser fields, emit radiation of frequency multiple of that of the driving field. HOHG has been widely studied in strong field physics [1,2], and is well explained by the three step semiclassical mechanism [3–5]. According to this mechanism, the electron first tunnels through the potential barrier formed by the combined Coulomb and laser fields, then it is accelerated by the laser field, and later driven back for a recollision with the core. Upon this recollision, the returning electron wave packet recombines with the core, leading to harmonic radiation.

Theoretical and experimental work on HOHG has been mostly devoted to atoms. The study of molecules is at the early stages, and is more challenging and richer in physics, due to additional complexity and symmetries. Experiments have shown that the molecular orientation w.r.t. the laser polarization axis strongly influences ionization [6] and harmonic generation (HG) [7]. Theoretical studies of effects of molecular orientation on HG require solving the time-dependent Schrödinger equation (TDSE); so far, only static nuclei model potentials [8,9] or two-dimensional (2D) models [10] have been used. Other studies [11] explored the zero-range potential and the strong field approximation. In this paper, we solve the 3D static nuclei TDSE for H_2^+ in a laser pulse with arbitrary oriented linear polarization.

For molecules (in contrast to atoms), the returning wave packet in the semiclassical picture of HOHG encounters a core comprising two or more centers (nuclei), which are presumed to behave as pointlike sources, potentially leading to interferences in HG [10] and in ATI spectra [12]. Also, depending on the molecular orientation, the nuclei may not "see" the same returning wave packet, and there may be a delay between their recollision times. Recent 2D simulations in two dimensions have found that harmonic spectra of H_2^+ and H_2 exhibit a minimum, whose location could be approximately predicted by regarding it as resulting from interferences between point sources located at the nuclei [10,12]. In this paper, we develop a 3D approach that yields the contribution of each nucleus to the harmonic spectrum of H_2^+, thus the role of each nucleus and interference effects are exhibited quantitatively. We show that each nucleus is a source of harmonic radiation, whose spectrum has features similar to that of an atom, except the presence of both *odd* and *even* harmonics. We find that the interference of radiation originated from the two nuclei leads not only to a minimum in the harmonic spectrum [10], but also to a destruction of even harmonics over a wide range of harmonics. We also show that upon recollision of the returning wave packet with the molecular core, the nucleus that is encountered first by the wave packet emits more intense harmonics than the other.

The TDSE for H_2^+ in a laser field is

$$i(\partial/\partial t)\Psi(\mathbf{r},t) = [H + \mathbf{A}(t)\cdot\mathbf{p}]\Psi(\mathbf{r},t), \tag{1}$$

where $H=\mathbf{p}^2/2+V(r)+1/R$ is the bare Hamiltonian, and $\mathbf{p}$ is the electron momentum. We fix the two nuclei along the z axis with internuclear distance R. The Coulomb potential experienced by the electron is $V(r)=V_1(r)+V_2(r)$, where $V_j(r)=-1/r_j$ ($j=1$ and 2) is the potential due to the nucleus j. $r_1=|\mathbf{r}+\mathbf{R}/2|$ and $r_2=|\mathbf{r}-\mathbf{R}/2|$ denote the distances of the electron with respect to the nuclei 1 and 2, respectively. The vector potential of the laser is $\mathbf{A}(t)=A_0 f(t)\sin(\omega_0 t)\hat{e}$, where A_0 is the maximum amplitude, ω_0 is the laser frequency, $f(t)$ is the pulse envelop, and $\hat{e}$ is the unit vector along the laser polarization axis. This axis is chosen in the yz plane, i.e., $\hat{e}=\sin(\chi)\hat{e}_y+\cos(\chi)\hat{e}_z$, where χ is the angle between the z axis and the laser polarization axis. $\hat{e}_y$ and $\hat{e}_z$ are unit vectors along the y and z axes.

To solve the TDSE (1), we use prolate spheroïdal coordinates (ξ,η,ϕ), where $\xi=(r_1+r_2)/R$, $\eta=(r_1-r_2)/R$, and ϕ is the azimuthal angle. The wave function is expanded in a complex basis as follows:

$$\Psi(\xi,\eta,\phi,t) = \sum_{m,\mu,\nu} a_{m\mu\nu}(t) U_\nu^m(\xi) V_\mu^m(\eta)(e^{im\phi}/\sqrt{2\pi}), \tag{2}$$

where $a_{m\mu\nu}(t)$ are time-dependent coefficients; and where $U_\nu^m(\xi)=N_\nu^m e^{-\beta R(\xi-1)}(\xi^2-1)^{|m|/2}L_{\nu-|m|}^{2|m|}(2\beta R(\xi-1))$, and $V_\mu^m(\eta)$

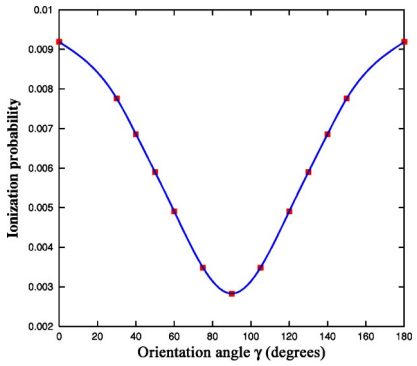

FIG. 1. Ionization probability of H_2^+ vs its orientation angle χ with respect to the laser polarization axis. The squares are the calculated data, the line is drawn to guide the eye.

$=M_\mu^m P_\mu^m(\eta)$. m is the electron's angular momentum projection onto the z axis: $m=0,\pm1,\pm2,\ldots,\pm m_{\max}$; $\mu=|m|,|m|+1,\ldots,|m|+\mu_{\max}$; and $\nu=|m|,|m|+1,\ldots,|m|+\nu_{\max}$. $L_p^q(x)$ and $P_p^q(x)$ denote associated Laguerre and Legendre functions, respectively. N_ν^m and M_μ^m are normalization constants.

Implementing complex scaling in spheroidal coordinates consists of using a complex nonlinear parameter $\beta=|\beta|e^{-i\theta}(0<\theta<\pi/2)$, so that the basis functions $U_\nu^m(\xi)$ behave asymptotically as outgoing waves [13]. This asymptotic behavior is crucial for time-propagation, because it prevents reflections at the boundaries of the region described by the wave function [14]. Projected in the basis (2), the TDSE takes the matrix form $i\partial\mathbf{S}\Psi/\partial t=[\mathbf{H}+A(t)\mathbf{D}]\Psi$, where Ψ is a vector representation of the wave function. **S**, **H**, and **D**

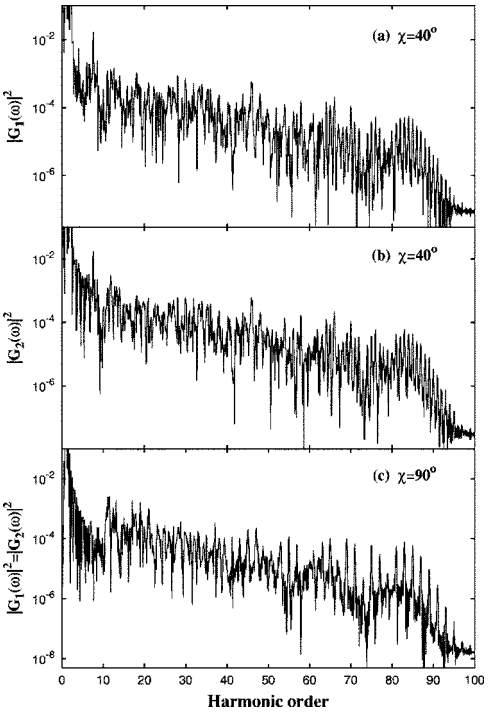

FIG. 2. Harmonic spectra (in arb. units) originating from the nucleus 1 of H_2^+ (i.e., $|G_1(\omega)|^2$), and from the nucleus 2 of H_2^+ (i.e., $|G_2(\omega)|^2$), for various orientation angles χ: (a) $|G_1(\omega)|^2$ for $\chi=40°$; (b) $|G_2(\omega)|^2$ for $\chi=40°$; (c) $|G_1(\omega)|^2=|G_2(\omega)|^2$ for $\chi=90°$.

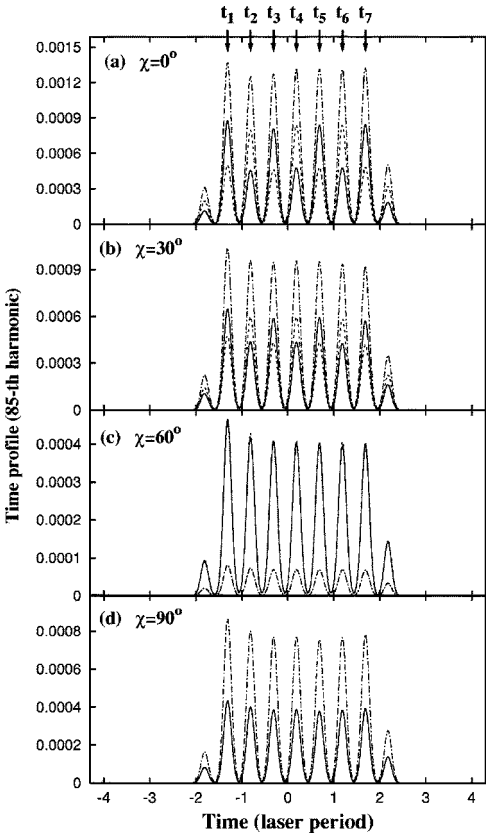

FIG. 3. Time profiles (in arb. units) of the 85th harmonic emitted by the nucleus 1 (solid line), and by the nucleus 2 (dashed lines) of H_2^+, for orientation angles χ shown. Both are identical for $\chi=90°$. The dot-dashed line is the profile for the 85th harmonic from H_2^+ (interferences included).

denote the overlap, the bare Hamiltonian, and the dipole matrices, respectively. We use a Runge-Kutta method to propagate the TDSE, starting from the ground state obtained by diagonalizing **H**. This yields energies and wave functions, thus providing a test for the accuracy of the basis expansion. With basis parameters used in this work, the energies of the ground state and of more than 1000 lowest excited states are obtained with an accuracy better than 10^{-10}. Details of our numerical approach will be published separately.

Results discussed in this paper have been obtained with the basis parameters: $|\beta|=0.2$, $\theta=0.1$, $m_{\max}=30$, $\mu_{\max}=30$, and $\nu_{\max}=70$, leading to about 135 000 basis functions. We use a laser pulse with $\omega_0=0.057$ a.u.(800 nm), and peak intensity 5×10^{14} W/cm^2. The pulse is turned on and off linearly over three laser periods, and kept at constant intensity for four laser periods, for a total of ten laser periods (26 fs). The internuclear distance $R=2$ a.u. is used.

The harmonic spectrum $S(w)\propto|A_{\hat{e}}(\omega)|^2$, where

$$A_{\hat{e}}(\omega)=\int e^{i\omega t}\langle\Psi(t)|\hat{e}\cdot[\nabla V(r)+\mathbf{E}(t)]|\Psi(t)\rangle dt, \qquad (3)$$

and $\mathbf{E}(t)=-\partial\mathbf{A}/\partial t$ is the electric field of the laser. When the ground state is not significantly depleted, as in this work, then $\langle\Psi(t)|\Psi(t)\rangle\approx1$, which leads to $A_{\hat{e}}(\omega)\approx G(w)$

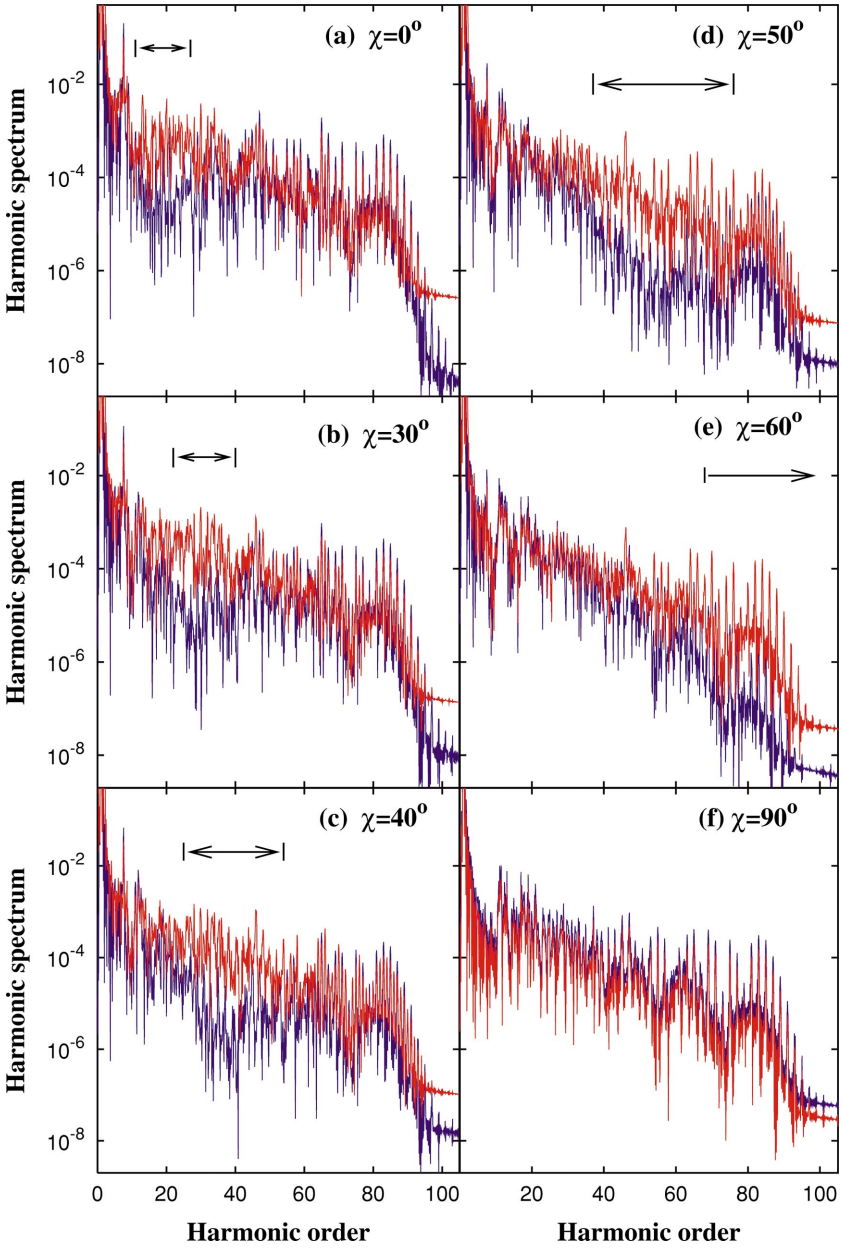

FIG. 4. (Color) Full harmonic spectrum $|G(\omega)|^2$ (blue curve) of H_2^+, and harmonic spectrum $|G_1(\omega)|^2+|G_2(\omega)|^2$ (red curve) of H_2^+ without account of interferences. The arrows cover the set of harmonics that are suppressed by at least one order of magnitude due to interferences. High-order harmonic generation from two-center molecules. Time-profile analysis of the number of contributions.

$+\hat{e}\cdot\int e^{i\omega t}\mathbf{E}(t)dt$, where $G(\omega)\equiv\int e^{i\omega t}\langle\Psi(t)|\hat{e}\cdot\boldsymbol{\nabla}V(r)|\Psi(t)\rangle dt$. The contribution of $\mathbf{E}(t)$ to $A_{\hat{e}}(\omega)$ is localized around the first harmonic. Thus, nearly all features of the HOHG spectrum are determined by $|G(\omega)|^2$. We hereafter refer to $|G(\omega)|^2$ as the harmonic spectrum. Because $V(r)=V_1(r)+V_2(r)$, one may introduce $G_j(\omega)\equiv\int e^{i\omega t}\langle\Psi(t)|\hat{e}\cdot\boldsymbol{\nabla}V_j(r)|\Psi(t)\rangle dt$, where $j=1$ and 2, so that $G(\omega)=G_1(\omega)+G_2(\omega)$. Since $G_j(\omega)$ is the analog of $G(\omega)$ for the nucleus j, it is natural to interpret $|G_j(\omega)|^2$ as the harmonic spectrum originating from the nucleus j. Although it is not obvious how to measure $|G_j(\omega)|^2$, their evaluation sheds light on very interesting physics, discussed below.

The ionization probability $P(T)$ is given by $P(T)=1-\Sigma_j\langle\Psi_j|\Psi(T)\rangle$, where the sum runs over all bound states $|\Psi_j\rangle$, and where $|\Psi(T)\rangle$ is the wave function at the end of the pulse at time $t=T$. $P(T)$ vs the angle χ, shown in Fig. 1, indicates that the ionization is maximum for the parallel orientation ($\chi=0°$), and decreases with increasing angle χ to reach a minimum for the perpendicular orientation ($\chi=90°$).

Figure 2 shows the spectra $|G_1(\omega)|^2$ and $|G_2(\omega)|^2$ originating from the nuclei 1 and 2, for angles $\chi=40°$ and $\chi=90°$. These spectra look much like atomic spectra, with a cutoff that is independent of the angle χ and located at approximately the 85th harmonic. This agrees with the cutoff law $E_c\approx I_p+3.17U_p$ [3,4], where I_p is the ionization potential of H_2^+ and U_p the ponderomotive energy. However, a remarkable feature in Fig. 2 is the presence of both *odd* and *even* harmonics. This feature is present for all orientations, except for $\chi=90°$, and is due to a break of the inversion symmetry. Indeed, it is clear that the potential seen by the electron from one nucleus is not inversion symmetric for $\chi\neq 90°$. But for $\chi=90°$, this inversion symmetry holds, leading to only odd harmonics [Fig. 2(c)].

Time profiles of harmonics emitted by each nucleus of H_2^+ and by the H_2^+ molecule are shown in Fig. 3, for various

angles χ. These profiles are obtained via a Gabor transform [15] of $G_j(\omega)$ and $G(\omega)$, using a Gaussian window function having a full width at half maximum of $5\omega_0$ and centered at the 85th harmonic. All profiles show two peaks every laser period, indicating harmonic emission upon the two recollisions of the electron wave packet with the molecular core. The positions of the peaks are independent of the molecular orientation and are separated by half the laser period.

We now focus on the case $\chi=0°$ in Fig. 3(a). The first major peak in the profile occurs at time $t_1\approx-1.31$ (in units of the laser period); a classical analysis indicates that at this time, the returning wave packet encounters nucleus 1 first, and nucleus 2 next [16]. One sees that there is an intensity asymmetry at $t=t_1$, as the intensity of the profile for nucleus 1 higher than that of nucleus 2. At the next peak in the profile at time $t_2\approx-0.81$, the wave packet encounters nucleus 2 first, and nucleus 1 next, leading to a more intense profile for nucleus 2 than for nucleus 1. For all orientations except $\chi\rightarrow90°$, this asymmetry exists, and the role played by the nuclei 1 and 2 alternate from one recollision to the next. This clearly indicates that every half-cycle, high order harmonics are emitted predominantly by the nucleus that experiences the first recollision with the returning electron wave packet. In fact, after recolliding with the first nucleus it encounters, the returning electron wave packet that reaches the second nucleus is attenuated mainly by its scattering off the first nucleus. This is evidence that the nuclei screen each other from the returning wave packet. This screening gradually decreases as χ increases from 0° to 90°. This is illustrated in Fig. 3, where the asymmetry in the intensity of harmonic profiles of the nuclei at each recollision decreases as $\chi\rightarrow90°$. Note that the profile for H_2^+ in Fig. 3(c) is strongly suppressed, compared to that of the two nuclei. As shown in Fig. 4(e), this is due to a strong destructive interference in the vicinity of the 85th harmonic.

It follows from the above that each nucleus is a source of harmonic radiation, and that one may write the spectrum of H_2^+ as $|G(\omega)|^2=|G_1(\omega)|^2+|G_2(\omega)|^2+2\,\mathrm{Re}[G_1(\omega)G_2^*(\omega)]$. Thus, we identify $2\,\mathrm{Re}[G_1(\omega)G_2^*(\omega)]$ as the interference term, and $|G_1(\omega)|^2+|G_2(\omega)|^2$ as the harmonic spectrum of H_2^+ without account of interferences. We have plotted $|G(\omega)|^2$ and $|G_1(\omega)|^2+|G_2(\omega)|^2$ in Fig. 4 for various angles χ. For each angle, a direct comparison of the two plots allows to assess the influence of interferences in the spectrum. As expected from Fig. 2, the spectra obtained without inclusion of the interference term exhibit both odd and even harmonics, except for $\chi=90°$ [Fig. 4(f)]. The inclusion of the interference term leads to a cancellation of even harmonics [see Figs. 4(a)–4(e)]. In fact, one of the consequences of adding the interference term is to restore the overall inversion symmetry of the system, leading to only odd harmonics. For $\chi=90°$, even harmonics are absent, as discussed previously, and $|G(\omega)|^2=4|G_1(\omega)|^2=4|G_2(\omega)|^2$, i.e., there are only constructive interferences. Having in mind the semiclassical picture of HOHG, it is clear that for $\chi=90°$, the two nuclei see the same tunneling and returning wave packet, which recollides with the two nuclei simultaneously. Thus, both nuclei simultaneously emit radiation of the same intensity, frequency, and phase, which simply add to each other.

It also appears from Fig. 4 that interferences lead to a strong suppression (up to two orders of magnitude) of a set of consecutive harmonics, leading to a minimum in the harmonic spectrum. With increasing angle χ the size of this set of strongly suppressed harmonics increases, and the center of this set moves to higher harmonics.

In conclusion, we have solved the 3D TDSE for a two-center molecule having one active electron, in an intense arbitrary polarized laser pulse. We have shown that each nucleus of H_2^+ is a source of harmonic radiation, whose spectrum is similar to that of an atom, besides the presence of both *odd* and *even* harmonics. Interference of harmonic radiation emitted by each nucleus leads to a minimum in the harmonic spectrum of H_2^+, and to a destruction of even harmonics. Every half-cycle, for angles $\chi\neq90°$ for which the nuclei screen each other from the returning electron wave packet, the nucleus that experiences the first recollision with the wave packet emits more intense harmonics than the other. Finally, the interference of harmonics emitted from each nucleus occurs over a wide spread of harmonic orders, thus implying that many electron trajectories probably contribute to the spectrum. The mathematics of the interference pattern is currently investigated in detail [17].

[1] P. Salières *et al.*, Adv. At., Mol., Opt. Phys. **41**, 83 (1999).
[2] T. Brabec and F. Krausz, Rev. Mod. Phys. **72**, 545 (2000).
[3] K. C. Kulander, K. J. Schafer, and J. L. Krause, in *Super Intense Laser Atom Physics*, edited by B. Piraux (Plenum, New York, 1993), Vol. 316, p. 95.
[4] P. B. Corkum, Phys. Rev. Lett. **71**, 1994 (1993).
[5] M. Lewenstein *et al.*, Phys. Rev. A **49**, 2117 (1994).
[6] I. V. Litvinyuk *et al.*, Phys. Rev. Lett. **90**, 233003 (2003).
[7] R. Velotta *et al.*, Phys. Rev. Lett. **87**, 183901 (2001).
[8] H. Yu and A. D. Bandrauk, J. Chem. Phys. **102**, 1257 (1995).
[9] M. Lein *et al.*, Phys. Rev. A **67**, 023819 (2003).
[10] M. Lein *et al.*, Phys. Rev. Lett. **88**, 183903 (2002); Phys. Rev. A **66**, 023805 (2002).
[11] R. Kopold *et al.*, Phys. Rev. A **58**, 4022 (1998).
[12] T. Zuo, A. D. Bandrauk, and P. B. Corkum, Chem. Phys. Lett. **259**, 313 (1996).
[13] P. Froelich *et al.*, J. Phys. B **20**, 6173 (1987).
[14] S. D. Parker and C. W. McCurdy, Chem. Phys. Lett. **156**, 483 (1989); C. W. McCurdy and C. K. Stroud, Comput. Phys. Commun. **63**, 323 (1991).
[15] P. Antoine, B. Piraux, and A. Maquet, Phys. Rev. A **15**, R1750 (1995), and references therein.
[16] At the internuclear distance $R=2$ used in this work, the time delay between the recollisions of the returning wave packet with each nucleus is not visible in Fig. 3.
[17] G. Lagmago Kamta and A. D. Bandrauk (unpublished).